CTP synthase forms cytoophidia in archaea

Shuang Zhou[1,2,3], Hua Xiang[2,4] and Ji-Long Liu[1*]

[1]School of Life Science and Technology, ShanghaiTech University, Shanghai, China

[2]University of Chinese Academy of Sciences, Beijing, China

[3]Institute of Biochemistry and Cell Biology, Shanghai Institutes for Biological Sciences, Chinese Academy of Sciences, Shanghai, China

[4]State Key Laboratory of Microbial Resources, Institute of Microbiology, Chinese Academy of Sciences, Beijing, China

*Correspondence should be addressed to Ji-Long Liu (E-mail: liujl3@shanghaitech.edu.cn).

Abstract

CTP synthase (CTPS) is an important metabolic enzyme that catalyzes the rate-limiting reaction of de novo synthesis of the nucleotide CTP. Since 2010, a series studies have demonstrated that CTPS can form filamentous structures termed cytoophidia in bacteria and eukaryotes. However, it remains unknown whether cytoophidia exist in archaea, the third domain of life. Using *Haloarcula hispanica* as a model system, here we demonstrate that CTPS forms distinct intracellular compartments in archaeal cells. Under stimulated emission depletion (STED) microscopy, we find that those HhCTPS compartments are elongated filamentous structure, resembling cytoophidia in bacteria and eukaryotes. When *Haloarcula* cells cultured in low-salt medium, the occurrence of cytoophidia increases dramatically. Moreover, overexpression CTPS or glutamine analog treatment promote cytoophidium assembly in *H. hispanica.* Our study reveals that CTPS forms cytoophidia in all three domains of life, suggesting that forming cytoophidia is an ancient property of CTPS.

Running titles: Cytoophidia in archaea

Key words: archaea; CTPS; cytoophidium; *Haloarcula hispanica*

Author Summary

CTP synthase (CTPS), as a textbook molecule, has been studied biochemically for almost 70 years. It catalyses the last step of making up the nucleotide CTP. Since biochemical properties and the regulatory mechanisms of CTPS were thoroughly studied in the past decades, it came as a surprise when a new feature of CTPS was revealed in 2010. Multiple studies reveal that CTPS can form snake-shaped structures termed cytoophidia in bacteria and eukaryotes. However, it is not clear whether cytoophidia exist in archaea, the third domain of life. Here we use halophilic archaeon *Haloarcula hispanica* as a model and show that CTPS can form defined structures in archaea. Using super resolution microscopy, we confirm that those CTPS-containing structures are elongated filaments, similar to cytoophidia described in bacteria and eukaryotic cells. Therefore, this study demonstrates that CTPS forms cytoophidia not only in bacteria and eukaryotes, but also in archaea.

Introduction

CTP (cytidine triphosphate) is the basic building blocks of RNA and DNA and key precursor in the biosynthesis of membrane phospholipids[1]. The synthesis of the CTP is the last committed step in pyrimidine nucleotide de novo synthesis catalyzed by CTP synthase (CTPS)[2]. This catalytic reaction includes the ATP-dependent phosphorylation on C-4 position of UTP to form intermediate 4-phosphoryl UTP which is reacted with ammonia from glutamine hydrolysis to generate CTP[3, 4]. GTP activates glutamine hydrolysis by allosterically bounding to CTPS to form a covalent glutaminyl enzyme intermediate[5, 6]. The product CTP is a competitive inhibitor of the enzyme which is critical to maintain the intracellular CTP level[7, 8].

Compartmentation is the process of formation of cellular compartments which play a key role in homeostasis[9]. Compartments are often defined as membrane enclosed regions such as mitochondria, chloroplasts and so on[10]. While compartmentation is also found in protein-based membraneless organelles such as purinosomes[11] and Cajal bodies[12]. In 2010, CTPS was found to compartment into filamentous structures in

Drosophila. These structures are termed cytoophidia (cellular snakes in Greek)[13]. Since then, independent studies have dicovered that CTPS can form cytoophidia in bacteria (*E. coli* and *Caulobacter crescentus)*[14], and eukaryotes such as budding yeast, fission yeast, human cells and plant cells[14-19]. The phenomenon that CTPS forms cytoophidia is very conservative across bacterium and eukaryotes.

Life can be divided into three domains: archaea, bacteria and eucarya[20]. Several studies have found evidence of CTPS-forming cytoophidia in bacteria and eukaryotes, which raises a very interesting question. We would like to know if this structure exists in archaea. The reason for this problem is that many archaea survive in extreme environments in which most microorganisms are not able to survive. So we want to ask the following three questions: 1) Can CTPS form intracellular structures in archaea? 2) Under what conditions can the intracellular structure be formed? 3) What is the relationship between the formation of intracellular structures and the physiology of archaea?

To answer those questions, we chose the halophilic archaeon *Haloarcula hispanica (H. hispanica)* ATCC 33960 as a model

system. *Haloarcula species* are salt loving extremophilic halophiles requiring 1.5 M to saturated salt concentration for growth[21, 22]. *H. hispanica* was isolated from a solar saltern in Spain, and a classic model in archaeal research[23]. *H. hispanica* can survive well in a medium containing optimal NaCl concentration at 3.5-4.2 M. It grows slowly in the case of low salt. Minimum Mg^{2+} concentration requires 0.005 M. The optimum growth temperature is 35-40°C and the pH range for growth is 6-8 with the optimal pH at 7.0[24].

Results

CTPS forms cytoophidia in *H. hispanica*

CTPS is evolutionarily conserved among all three domains of life: archaea, bacteria and eukarya (**Figure 1**). *H. hispanica* CTP synthase (HhCTPS) gene is located in Chromosome I[25], HhCTPS contains two conserved regions: N terminal region (residues 16 to 277, ligase domain) and C terminal region (residue 303 to 535, glutaminase, Type 1 glutamine amidotransferase). There is a significant similarity between CTP synthase from *H. hispanica* and proteins from *Thermus thermophiles*, Human, *Saccharolobus solfataricus*, *Drosophila*, *E. coli*, *Mycobacterium tuberculosis*, *Saccharomyces cerevisiae*, which share 46% - 53% sequence identity **(Figure 1; Figure S1)**.

In order to visualize the *H. hispanica* CTPS in *H. haloarcula*, we fused modified pSMRSGFP to the C-terminus of CTPS and visualized the distribution of HhCTPS-GFP (pSMRSGFP knock-in strain) under laser scanning confocal microscopy and super-resolution microscopy (**Figure 2a-c**). We found that CTPS is mostly diffusely distributed in normal conditions. Only a small number of cells can form foci (**Figure 2b**). The intracellular compartmentalized

foci were relatively small and it was difficult to determine the shape of those foci under conventional confocal microscopy.

We also wanted to see how the intracellular compartmentalized structures in *H. hispanica* differ from cytoophidia in bacteria and eukaryotes. Specifically, we wish to know whether the HhCTPS foci are completely circular or elongated. Under stimulated emission depletion (STED) microscopy, we observed that some HhCTPS-forming compartmentalized structures look like rod or dot under confocal are actually lengthened structures **(Figure 2c)**. Our results indicate that HhCTPS can form elongated filamentous structures in *H. hispanica*. Therefore, we conclude that HhCTPS has filament-forming property. In other words, cytoophidia exist in *H. hispanica*.

H. hispanica* CTPS forms cytoophidia in *E. coli

To determine whether HhCTPS can form cytoophidia in other species independent of its own intracellular environment, we expressed mCherry-labeled HhCTPS in *E. coli*. We found that HhCTPS can form cytoophidia in *E. coli* **(Figure 2d)**. However, cytoophidia formed by HhCTPS were in these two species are somewhat different from those formed by EcCTPS. In *E. coli* cells, homogenous EcCTPS forms longer cytoophidia in more cells than

heterogenous HhCTPS. These differences may be due to species-specific factors required for cytoophidium assembly. Nevertheless, our study demonstrates that Haloarcula CTPS has the ability to form cytoophidia in *E. coli*.

A glutamine analog promotes cytoophidium assembly in *H. hispanica*

Eukaryotic CTPS uses glutamine as a substrate. It was found that 6-diazo-5-oxo-l-norleucine (DON), an analog of glutamine, inhibits CTPS activity by irreversibly binding to its glutamine amidotransferase domain. Meanwhile DON promotes cytoophidium assembly in *Drosophila* and human cells[26, 27], but inhibits the formation of cytoophidia in bacteria[14]. To understand how DON affects HhCTPS in *H. hispanica*. *H. hispanica* cells were cultured in medium supplemented with DON. We observed that DON-treatment induces cytoophidium assembly in *Haloarcula hispanica* cells **(Figure S2)**. Our data indicate that the effect of DON on HhCTPS-forming cytophidia is similar to that on *Drosophila* and human CTPS, but different from that on bacteria CTPS.

Low salinity induces cytoophidium formation in *H. hispanica*

Next we want to know how HhCTPS-forming cytoophidia are related

to the physiological characteristics of *H. hispanica*. We cultured *H. hispanica* under different conditions. We found that the *H. hispanica* cells cultured in low-salt medium (1.5 M NaCl AS168) became rounded like a balloon from the original polymorphism (rod, circle, square, triangle, irregular shapes) due to osmotic pressure **(Figure 3a-d)**. In comparison, the cell shape became bigger and longer under DON treatment **(Figure 3)**. It seemed that cell division was suppressed because of the inhibition of HhCTPS by DON.

Surprisingly, HhCTPS can form a large number of intracellular structures under the low-salt condition (1.5M NaCl AS168) **(Figure 4a,b)**. Under low-salt condition, the *H. hispanica* cells grew very slowly, almost stopping growth **(Figure 4c,d)**. After cultivating about 3 days in 1.5M NaCl AS168 medium, HhCTPS-GFP cells were transferred to normal AS168 medium, Cells grown again but the abundance of HhCTPS compartmentalized structure was decreased. If HhCTPS-GFP cells continued maintaining in low salinity medium, it still kept growth cessation with higher abundance of compartmentalized structure **(Figure 4e-h)**. Therefore, low salinity could not support normal cell growth of halophiles. Salt shortage triggered Hhctps compartmentalization, which might be a repository store enzymes to keep cell a static state.

Using STED, we observed that the compartmentalized structures in cells cultured in low-salt medium exhibited an elongated shape **(Figure S3)**. The lengths of cytoophidia were significantly increased in DON-treated cells **(S3b, c Fig)**.

Overexpressing *Haloarcula* CTPS promotes cytoophidium formation

We wonder whether the level of CTPS has an effect on cytoophidium formation. Cytoophidia were induced in many *H. hispanica* cells when CTPS were overexpressed **(Figure 5a)**. STED images showed that HhCTPS-overexpression-induced cytoophidia were indeed elongated structures **(Figure 5b)**. Moreover, the formation of cytoophidia changes with the growth phases of archaea **(Figure 5c,d)**. The number of cytoophidia in the early stage of growth was reduced, but the volume of each cytoophidium was large. The abundances of cytoophidia in the logarithmic phase and subsequent growth phases were almost unchanged, but the cell size of cytoophidium decreased at first and increased later **(Figure 5e,f)**.

Uracil deprivation affects cytoophidium formation in *H. hispanica*

The uracil auxotrophic (*pyrF* deleted) strain DF60 was used to construct HhCTPS-GFP[17]. The functional *pyrF* gene could encode orotidine-50-phosphate decarboxylase that catalyzed a uracil analog 5-fluoroorotic acid (5-FOA) to toxic form (5-fluorouracil)[28]. The uracil auxotrophic strain DF60 need uracil supply to support normal physiological function. *The* yeast extract-subtracted AS168 medium was used to screen *pyrF*-expressing plasmids [29]. Uracil is one of the four nucleobases in the nucleic acid of RNA, and likes CTP, is a key component of RNA synthesis. In order to investigate whether the shortage of uracil affects the formation of HhCTPS cytoophidia, we cultured HhCTPS-GFP in yeast extract-subtracted AS168 medium. We found that HhCTPS also formed a number of cytoophidia **(Figure 6a,b)** which is elongated structure under STED microscopy **(Figure 6c).** Moreover, the growth curve of HhCTPS-GFP indicated that the growth of *H. hispanica* is inhibited in yeast extract-subtracted AS168 medium **(Figure 6d)**.

Discussion

In summary, we found that CTPS can form cytoophidia in *H. hispanica*. Our study demonstrates that CTPS forms cytoophidia not only in bacteria and eukaryotes, but also in archaea. Cytoophidia exist in all three domains of life, suggesting that forming cytoophidia is an ancient and fundamental property of CTPS. Furthermore, we find that environmental stress such as low salt condition can promote cytoophidium assembly in *H. hispanica*. We speculate that forming cytoophidia help *Haloarcula* cells adapting detrimental environment and increasing their survival.

Therefore, our model is that CTPS may be mostly diffuse under normal circumstances. However, in the case of low salt, CTPS can aggregate to form cytoophidia. Cytoophidia formed in this case may provide an environment to sequester the enzymatic activity of CTPS to protect the metabolic activity of the archaea. We transferred the low-salt culture of *H. hispanica* cells to normal medium and found that cytoophidia disappeared again. This phenomenon is consistent with that in eukaryotes.

Haloarcula is one example of the archaea. Our work shows that CTPS can form cytoophidia not only in eukaryotes and bacteria, but also in archaea. This work and studies in several laboratories including us in the first decade of the cytoophidium field indicate that filament-forming is an ancient and evolutionarily conservative phenomenon. In order to understand more about the role of the cytoophidia formed by CTPS in archaea, it is necessary to further explore in other archaea such as thermophiles and methanogens.

Material and Methods

Strains and growth conditions

The strains used in this study are listed in **Supplementary Table S1**. *Escherichia coli* was grown in Luria-Bertani medium at 37°C[30], with ampicillin at a final concentration of 100 μg/ml. The uracil auxotrophic (pyrF deleted) strain DF60 [29] and its derivatives were cultured at 37°C in AS168 medium (per liter, 200 g NaCl, 20 g $MgSO_4 \cdot 7H_2O$, 2 g KCl, 3 g trisodium citrate, 1 g sodium glutamate, 50 mg $FeSO_4 \cdot 7H_2O$, 0.36 mg $MnCl_2 \cdot 4H_2O$, 5 g Bacto casaminoacids, 5 g yeast extract, pH 7.2) that added uracil at a final concentration of 50 mg/l[31], 1.5M NaCl AS168 medium (per liter, 88g NaCl, other components are same with AS168), DON was adding when necessary. 15% Agar was adding for solid medium. Strains transformed with a suicide plasmid were cultured in yeast extract subtracted AS168[32].

Plasmid construction, transformation, and gene mutants

The plasmids used in this study are listed in **Supplementary Table S1** and primers used in this study are listed in **Supplementary Table S2**. For knock-in of pSMRSGFP in *H. hispanica* ATCC 33960, a 729-bp DNA fragment of pSMRSGFP gene with linker

(AGSAA)[33], a 663-bp DNA fragment at the 3 region of the HhCTPS gene containing a BamH I site at 5′ end and a 673-bp DNA fragment located downstream of the HhCTPS operon containing a Kpn I site at 3′ end were amplified by primer pairs HhCTPS-C-GFP-F / HhCTPS-C-GFP-R , HhCTPS-C-UF/ HhCTPS-C-UR and HhCTPS-C-DF/ HhCTPS-C-DR (**Supplementary Table S2**) from plasmid pWL502-GFP and genome. These three DNA fragments were linked and inserted into the suicide plasmid pHAR (predigested with BamHI and KpnI), and transfer into DF60 cells to knock in PSMRSGFP by the pop-in/pop-out method described previously[29]. The expression plasmid pWL502[31] was used to overexpress HhCTPS-GFP. DNA fragment of HhCTPS with PSMRSGFP was amplified form HhCTPS-GFP knock-in strain containing a BamH I site at 5′ end and a Kpn I site at 3′ end. This DNA fragment was inserted into plasmid pWL502 (predigest with BamHI and KpnI), and transfer into DF60 cells. pWL502-GFP (pWL502- pSMRSGFP) is used as control. All transformants were screened by PCR verification and confirmed by sequence analysis.

Heterogeneous expression

For heterogeneous expression of HhCTPS in *E. coli*. DNA fragments of HhCTPS or EcCTPS operon with linker (GGGS) and

mCherry gene were amplified by primer pairs ECCTPS-F / ECCTPS-R, mCherry-F / mCherry-R. Two DNA fragments were linked and inserted into plasmid pET28a, and transfer into Transetta (TRANSGEN BIOTECH). IPTG with a final concentration 1 μM was added when needed.

Preparation of fixed *H. hispanica*

Paraformaldehyde containing 20% NaCl was added to *H. hispanica* cell culture to give a final concentration of PFA of 4%. After fixing for 10 min at room temperature cells were spun down for 3 min at 6000 rpm/min, then washed once by basal salt solution (BSS; per liter, 200 g NaCl, 20 g $MgSO_4 \cdot 7H_2O$, 2 g KCl, and 3 g trisodium citrate). Store samples in BBS at 4°C.

Light microscopy

Cell suspension (2 μl) were mixed with 2 μl 1% low melting temperature agarose containing 18% BSW to avoid movement of the cells during imaging[32, 34]. Images were acquired under 63x objectives with DIC on a laser scanning confocal microscope (Leica SP8, Leica Microsystems CMS GmbH, Mannheim, Germany). For super-resolution imaging, stimulated emission depletion (STED) module (Leica TCS SP8 STED 3X) was used. The STED with GFP

was performed with the 592 nm continuous wave (CW). Images were captured using a 100x 1.4 NA oil objective. Instrument aberration and blurring was corrected with post-acquisition deconvolution using the Huygens Professional software. DIC and GFP epifluorescence images were analyzed using Fiji.

Growth analysis

H. hispanica cells were diluted in growth medium to a start optical density of approximately 0.1 at 600 nm (OD_{600nm}) (with growth medium used for blank). 5 ml cell cultures were incubated in 12 ml flasks or 20ml cell cultures were incubated in 100 ml flasks at 37°C with shaking (220 rpm). The OD_{600nm} was measured for three to ten days in each flask. The growth curves represent the average of three independent samples. The cell grown in 1.5 M NaCl AS168 was centrifuged for 3 min at 6000 rpm/min and the supernatant was remove. Then the cells were washed once with AS168 or 1.5 M NaCl AS168, finally transferred to AS168 or 1.5 M NaCl AS168 for continuing cultivation. The OD_{600nm} was measured every day in each flasks. For cell growth on the agar plate, 2 µl of culture in growth medium was inoculated into the subsurface of another growth medium agar plate, with up to four inoculations per plate from the same liquid culture. Plates were incubated in a closed plastic box at

42°C for 10 days, and then images of the plates were acquired using a camera.

Acknowledgments

We thank Junyu Chen, Luyao Gong and Xiaoming Li for technical assistance and the Molecular Imaging Core Facility at School of Life Science and Technology, ShanghaiTech University for providing the technical support.

References

1. Carman GM, Henry SA. Phospholipid biosynthesis in yeast. Annu Rev Biochem. 1989;58:635-69. Epub 1989/01/01. doi: 10.1146/annurev.bi.58.070189.003223. PubMed PMID: 2673019.
2. Koshland Jr D, Levitzki A. 16. CTP Synthetase and Related Enzymes. The Enzymes. 10: Elsevier; 1974. p. 539-59.
3. Lieberman I. Enzymatic amination of uridine triphosphate to cytidine triphosphate. J Biol Chem. 1956;222(2):765-75. Epub 1956/10/01. PubMed PMID: 13367044.
4. Long C, Koshland DE, Jr. Cytidine triphosphate synthetase. Methods Enzymol. 1978;51:79-83. Epub 1978/01/01. doi: 10.1016/s0076-6879(78)51014-8. PubMed PMID: 357909.
5. Levitzki A, Koshland DE, Jr. Role of an allosteric effector. Guanosine triphosphate activation in cytosine triphosphate synthetase. Biochemistry. 1972;11(2):241-6. Epub 1972/01/18. PubMed PMID: 4550559.
6. Long CW, Pardee AB. Cytidine triphosphate synthetase of Escherichia coli B. I. Purification and kinetics. J Biol Chem. 1967;242(20):4715-21. Epub 1967/10/25. PubMed PMID: 4862983.
7. Ostrander DB, O'Brien DJ, Gorman JA, Carman GM. Effect of CTP synthetase regulation by CTP on phospholipid synthesis in Saccharomyces cerevisiae. Journal of Biological Chemistry. 1998;273(30):18992-9001.
8. Endrizzi JA, Kim H, Anderson PM, Baldwin EP. Mechanisms of product feedback regulation and drug resistance in cytidine triphosphate synthetases from the structure of a CTP-inhibited complex. Biochemistry. 2005;44(41):13491-9.
9. Liu JL. The Cytoophidium and Its Kind: Filamentation and Compartmentation of Metabolic Enzymes. Annu Rev Cell Dev Biol. 2016;32:349-72. doi: 10.1146/annurev-cellbio-111315-124907. PubMed PMID: 27362644.
10. Diekmann Y, Pereira-Leal JB. Evolution of intracellular compartmentalization. Biochemical journal. 2013;449(2):319-31.
11. An S, Kumar R, Sheets ED, Benkovic SJ. Reversible compartmentalization of de novo purine biosynthetic complexes in living cells. Science. 2008;320(5872):103-6.
12. Cajal SR. Un sencillo metodo de coloracion seletiva del reticulo protoplasmatico y sus efectos en los diversos organos nerviosos de vertebrados e invertebrados. Trab Lab Invest Biol(Madrid). 1903;2:129-221.
13. Liu J-L. Intracellular compartmentation of CTP synthase in Drosophila. Journal of Genetics and Genomics. 2010;37(5):281-96. doi: 10.1016/s1673-8527(09)60046-1.
14. Ingerson-Mahar M, Briegel A, Werner JN, Jensen GJ, Gitai Z. The metabolic enzyme CTP synthase forms cytoskeletal filaments. Nat Cell Biol. 2010;12(8):739-46. Epub 2010/07/20. doi: ncb2087 [pii]
10.1038/ncb2087. PubMed PMID: 20639870.
15. Noree C, Sato BK, Broyer RM, Wilhelm JE. Identification of novel filament-forming proteins in Saccharomyces cerevisiae and Drosophila melanogaster. J Cell Biol. 2010;190(4):541-51. Epub 2010/08/18. doi: jcb.201003001 [pii]
10.1083/jcb.201003001. PubMed PMID: 20713603; PubMed Central PMCID: PMC2928026.
16. Carcamo WC, Satoh M, Kasahara H, Terada N, Hamazaki T, Chan JY, et al. Induction of

cytoplasmic rods and rings structures by inhibition of the CTP and GTP synthetic pathway in mammalian cells. PLoS ONE. 2011;6(12):e29690. Epub 2012/01/06. doi: 10.1371/journal.pone.0029690
PONE-D-11-11447 [pii]. PubMed PMID: 22220215; PubMed Central PMCID: PMC3248424.
17. Chen K, Zhang J, Tastan OY, Deussen ZA, Siswick MY, Liu JL. Glutamine analogs promote cytoophidium assembly in human and Drosophila cells. J Genet Genomics. 2011;38(9):391-402. Epub 2011/09/21. doi: 10.1016/j.jgg.2011.08.004. PubMed PMID: 21930098.
18. Daumann M, Hickl D, Zimmer D, DeTar RA, Kunz HH, Mohlmann T. Characterization of filament-forming CTP synthases from Arabidopsis thaliana. Plant J. 2018;96(2):316-28. doi: 10.1111/tpj.14032. PubMed PMID: 30030857.
19. Zhang J, Hulme L, Liu JL. Asymmetric inheritance of cytoophidia in Schizosaccharomyces pombe. Biol Open. 2014;3(11):1092-7. Epub 2014/11/02. doi: 10.1242/bio.20149613. PubMed PMID: 25361577; PubMed Central PMCID: PMCPMC4232767.
20. Woese CR, Kandler O, Wheelis ML. Towards a natural system of organisms: proposal for the domains Archaea, Bacteria, and Eucarya. Proceedings of the National Academy of Sciences. 1990;87(12):4576-9.
21. Madern D, Ebel C, Zaccai G. Halophilic adaptation of enzymes. Extremophiles. 2000;4(2):91-8.
22. Thombre RS, Shinde VD, Oke RS, Dhar SK, Shouche YS. Biology and survival of extremely halophilic archaeon Haloarcula marismortui RR12 isolated from Mumbai salterns, India in response to salinity stress. Scientific reports. 2016;6:25642.
23. Juez G, Rodriguez-Valera F, Ventosa A, Kushner DJ. Haloarcula hispanica spec. nov. and Haloferax gibbonsii spec, nov., two new species of extremely halophilic archaebacteria. Systematic and Applied Microbiology. 1986;8(1-2):75-9.
24. Garrity GM. Bergey's manual of systematic bacteriology: Volume one: the Archaea and the deeply branching and phototrophic bacteria: Springer Science & Business Media; 2012.
25. Liu H, Wu Z, Li M, Zhang F, Zheng H, Han J, et al. Complete genome sequence of Haloarcula hispanica, a Model Haloarchaeon for studying genetics, metabolism, and virus-host interaction. J Bacteriol. 2011;193(21):6086-7. doi: 10.1128/JB.05953-11. PubMed PMID: 21994921; PubMed Central PMCID: PMCPMC3194904.
26. Boeke JD, La Croute F, Fink GR. A positive selection for mutants lacking orotidine-5'-phosphate decarboxylase activity in yeast: 5-fluoro-orotic acid resistance. Molecular and General Genetics MGG. 1984;197(2):345-6.
27. Levitzki A, Koshland Jr D. Cytidine triphosphate synthetase. Covalent intermediates and mechanisms of action. Biochemistry. 1971;10(18):3365-71.
28. Calise SJ, Carcamo WC, Krueger C, Yin JD, Purich DL, Chan EK. Glutamine deprivation initiates reversible assembly of mammalian rods and rings. Cell Mol Life Sci. 2014;71(15):2963-73. Epub 2014/01/31. doi: 10.1007/s00018-014-1567-6. PubMed PMID: 24477477.
29. Liu H, Han J, Liu X, Zhou J, Xiang H. Development of pyrF-based gene knockout systems for genome-wide manipulation of the archaea Haloferax mediterranei and Haloarcula hispanica. J Genet Genomics. 2011;38(6):261-9. Epub 2011/06/28. doi: 10.1016/j.jgg.2011.05.003. PubMed PMID: 21703550.
30. CHONG L. Molecular Cloning. Science. 2001;292(5516):446-.
31. Cai S, Cai L, Liu H, Liu X, Han J, Zhou J, et al. Identification of the haloarchaeal phasin (PhaP)

that functions in polyhydroxyalkanoate accumulation and granule formation in Haloferax mediterranei. Appl Environ Microbiol. 2012;78(6):1946-52. Epub 2012/01/17. doi: 10.1128/AEM.07114-11. PubMed PMID: 22247127; PubMed Central PMCID: PMCPMC3298179.
32. Dyall-Smith M. The Halohandbook: protocols for haloarchaeal genetics. Haloarchaeal Genetics Laboratory, Melbourne. 2008;14.
33. Schmidt I, Pfeifer F. Use of GFP-GvpE fusions to quantify the GvpD-mediated reduction of the transcriptional activator GvpE in haloarchaea. Archives of microbiology. 2013;195(6):403-12.
34. Duggin IG, Aylett CH, Walsh JC, Michie KA, Wang Q, Turnbull L, et al. CetZ tubulin-like proteins control archaeal cell shape. Nature. 2015;519(7543):362.
35. Saitou N, Nei M. The neighbor-joining method: a new method for reconstructing phylogenetic trees. Molecular biology and evolution. 1987;4(4):406-25.

Figures 1-6; Figure legends

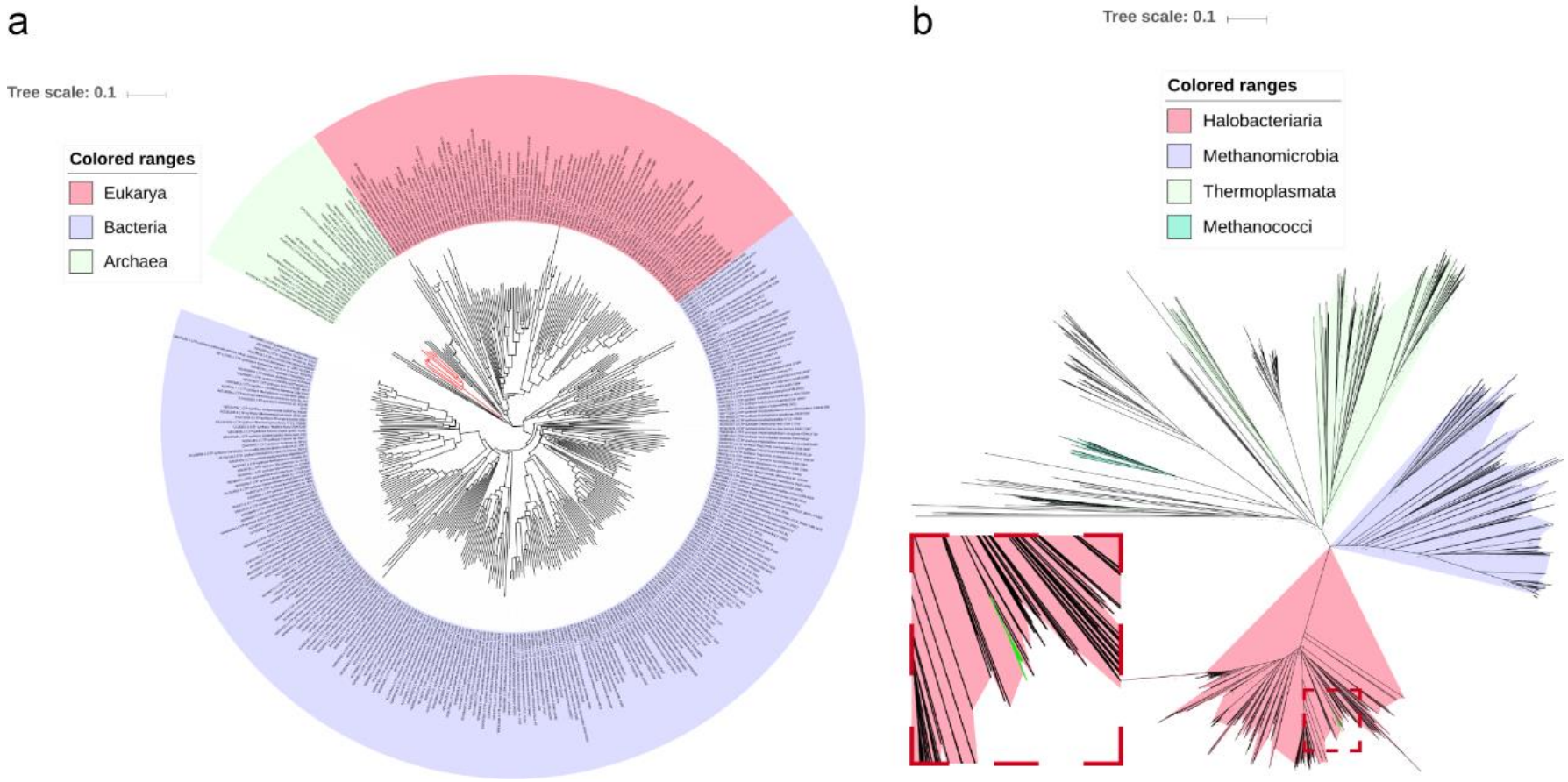

Figure 1

Fig 1. Neighbor-Joining[35] phylogenetic trees of CTP synthase proteins. a, Representative CTPS proteins from three life domains were selected and aligned for creating the phylogram. The CTPS proteins from halophiles were indicated in red. **b**, Almost all CTPS proteins in Euyarchaeota were used for building the phylogenetic tree which contain the clusters from Halobacteria, Methanomicrobia, Thermoplasmata, Methanococci and the like. The *Haloarcula* proteins were indicated in green.

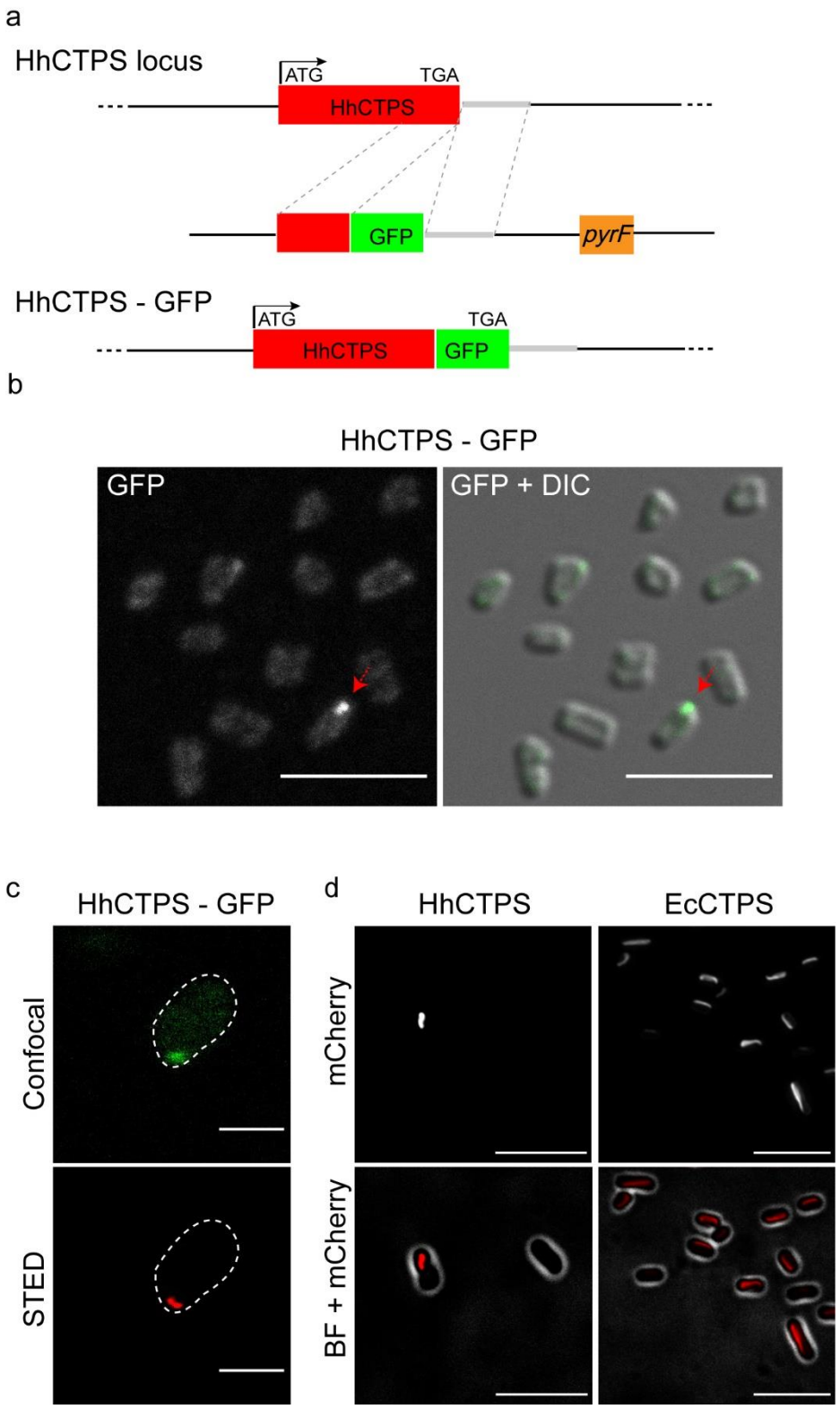
a
HhCTPS locus
ATG
TGA
HhCTPS
GFP
pyrF
HhCTPS - GFP
ATG
TGA
HhCTPS
GFP
b
HhCTPS - GFP
GFP
GFP + DIC
c
HhCTPS - GFP
Confocal
STED
d
HhCTPS
EcCTPS
mCherry
BF + mCherry

Figure 2

Figure 2. CTP synthase forms cytoophidia in *H. hispanica*. a, C-terminal targeting of endogenous *H. hispanica* CTPS (HhCTPS) with GFP. **b**, Confocal images of *H. hispanica* shows the compartmentalized capability of HhCTPS in the late log phase. Arrows point to the punctate structure. The DIC image represents the cell contour. **c**, In an *H. hispanica* cell, a compartmented CTPS structure (green, upper pane) observed under conventional confocal microscopy show elongated shape (red, lower panel) under stimulated emission depletion (STED) microscopy. This elongated filamentous structure in the archaeal cell resembles cytoophidia described in bacteria and eukaryotes. **d**, Heterologous expression of HhCTPS in *E. coli* demonstrates that HhCTPS can form cytoophidia in *E. coli.* Homogenous EcCTPS forms longer cytoophidia in more E. coli cells than heterogeneous HhCTPS. Both HhCTPS and EcCTPS are tagged with mCherry. *H. hispanica* is collected in late log phase, *E.coli* is collected in stationary phase. Scale bars, 5 μm in (b) and (d), 1 μm in (c).

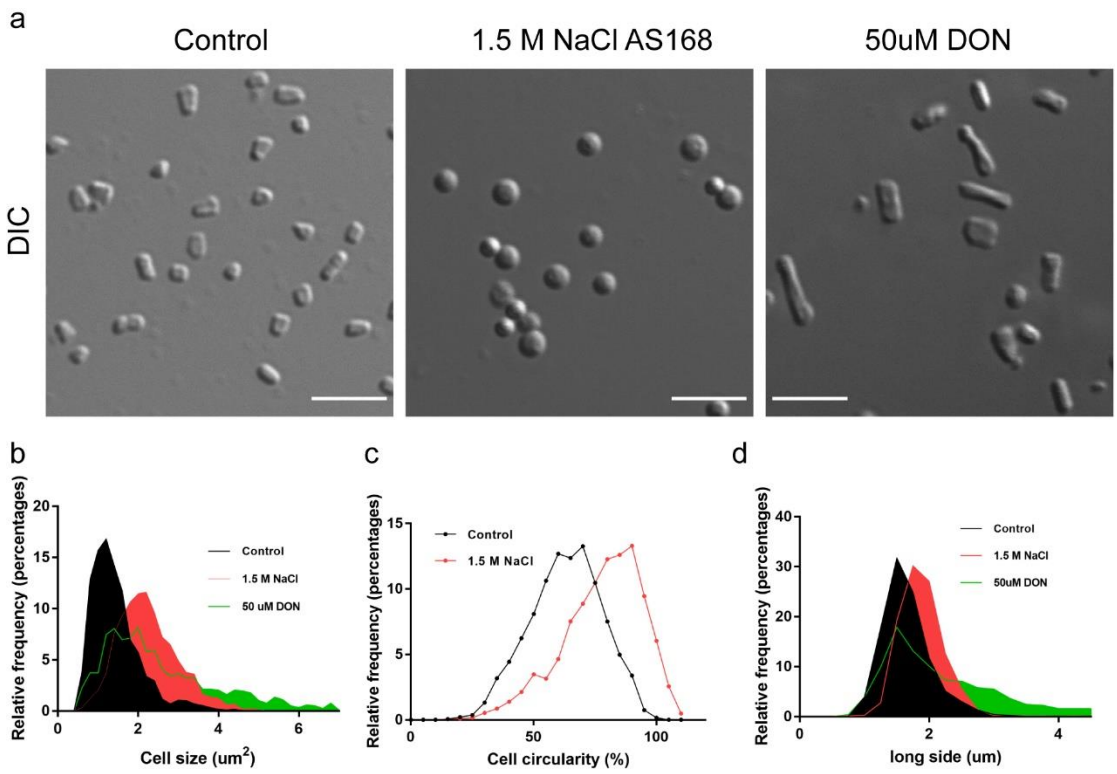

Figure 3

Figure 3. Low salinity and DON treatment change cell shapes in *H. hispanica*. a, DIC images of HhCTPS-GFP in normal condition, low salinity medium, DON treated medium on the third day of cultivation. **b**, **c**, **d**, Images were analyzed for cell size (**b**) cell circularity (**c**) and long side (The larger side of the minimum bounding rectangle) (**d**). n = 1897 in normal condition, 1181 in low salinity medium, and 1874 in DON treated medium. Mean ± SD. Scale bars, 5 μm.

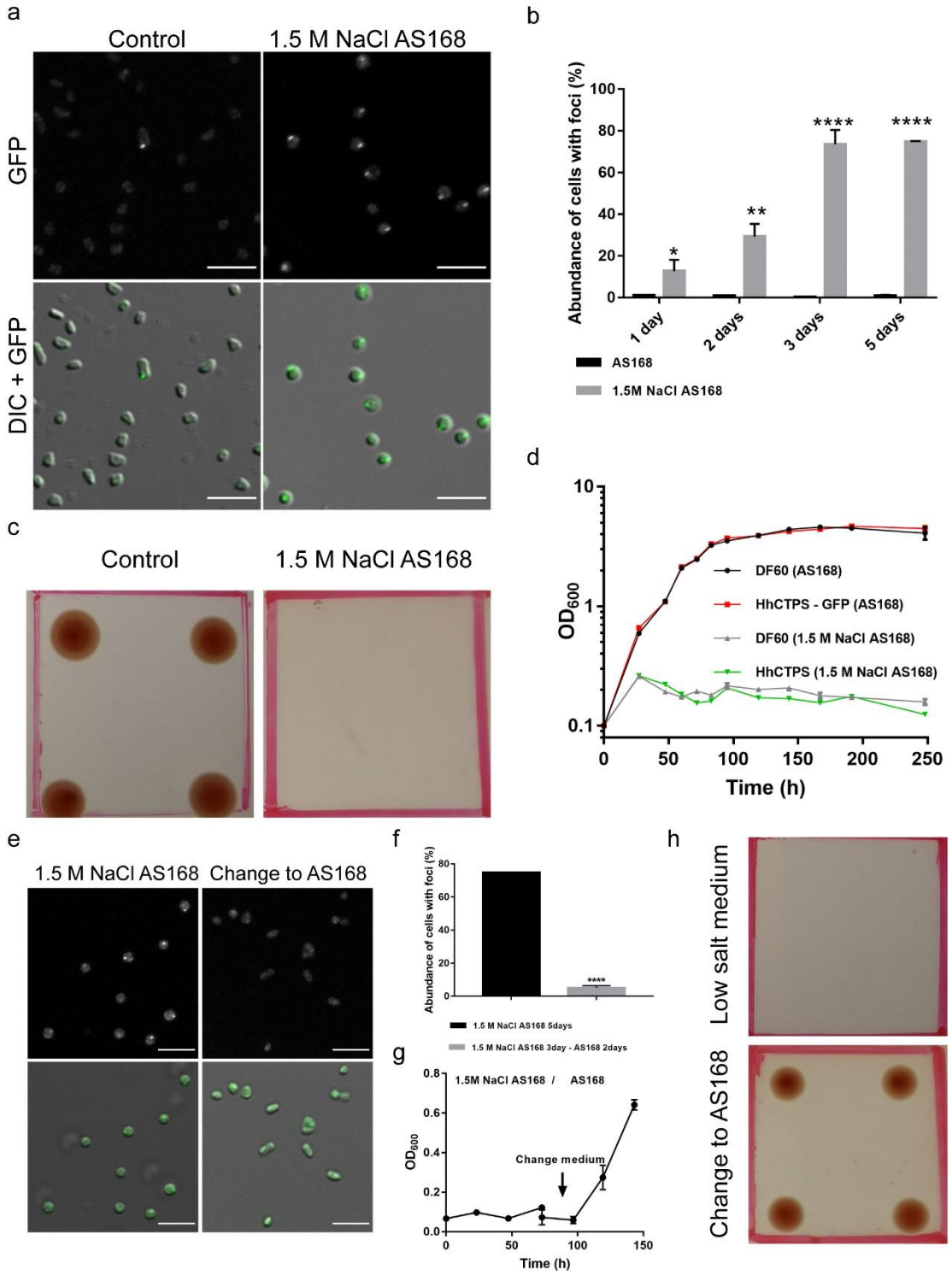
a
Control
1.5 M NaCl AS168
GFP
DIC + GFP
b
Abundance of cells with foci (%)
100
80
60
40
20
0
*
**
****
****
1 day
2 days
3 days
5 days
AS168
1.5M NaCl AS168
c
Control
1.5 M NaCl AS168
d
10
1
0.1
OD600
DF60 (AS168)
HhCTPS - GFP (AS168)
DF60 (1.5 M NaCl AS168)
HhCTPS (1.5 M NaCl AS168)
0
50
100
150
200
250
Time (h)
e
1.5 M NaCl AS168
Change to AS168
f
Abundance of cells with foci (%)
80
60
40
20
0
****
1.5 M NaCl AS168 5days
1.5 M NaCl AS168 3day - AS168 2days
g
1.5M NaCl AS168 / AS168
0.8
0.6
0.4
0.2
0.0
OD600
Change medium
0
50
100
150
Time (h)
h
Low salt medium
Change to AS168

Figure 4

Figure 4. Low salinity promotes the compartmentation of CTP synthase *H. hispanica*. a, Many compartmentalized structures appear in low salinity medium. **b**, Compartmentation ratio increases in low salt medium. Cells were collected at the first day (n = 1117 in AS168, 1553 in 1.5 M NaCl AS168), the second day (n = 2538 in AS168, 2180 in 1.5 M NaCl AS168), the third day (n = 3069 in AS168, 2118 in 1.5 M NaCl AS168) and the fifth day (n = 2639 in AS168, 1001 in 1.5 M NaCl AS168) of cultivation. Mean ± SD, *p <0.05, **p < 0.01, ****p < 0.0001. **c**, **d**, *H. hispanica* cannot grow normally in 1.5 M NaCl AS168 medium. There are red colonies in the AS168 plate (left pane), while no any colony in 1.5 M NaCl AS168 after 10days incubation (right pane)(**c**). The growth curve of *H. hiapanica* in this two different medium with a log scale for y axis (**d**). **e**, **f**, **g**, **h**, Salt supplementation recovers cell growth, meanwhile decreases the abundance of punctate structures. Confocal images (**e**), ratio of compartmentalized structure (**f**) (n = 1001 for low salinity culture, 1072 for recover culture), growth curve (**g**) and plates (**h**) shows salinity recovery diminishes compartmentation of HhCTPS-GFP. Positions of four repeat inoculations per plate are at the four corners of the red squares. Mean ± SD, ****p < 0.0001. Scale bars, 5μm.

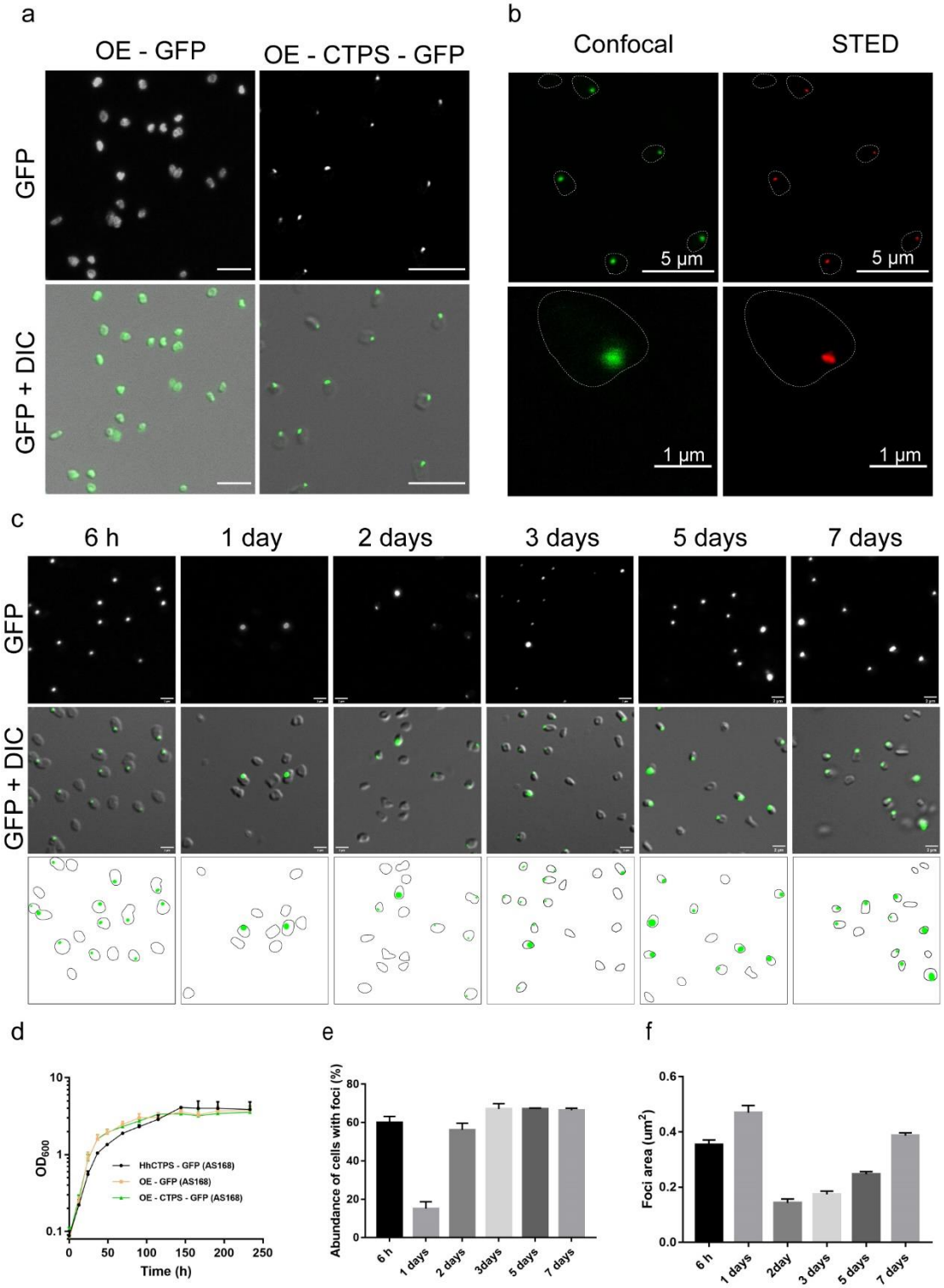
a
OE - GFP
OE - CTPS - GFP
GFP
GFP + DIC
b
Confocal
STED
5 µm
5 µm
1 µm
1 µm
c
6 h
1 day
2 days
3 days
5 days
7 days
GFP
GFP + DIC
d
OD600
Time (h)
HhCTPS - GFP (AS168)
OE - GFP (AS168)
OE - CTPS - GFP (AS168)
e
Abundance of cells with foci (%)
6 h
1 days
2 days
3days
5 days
7 days
f
Foci area (um2)
6 h
1 days
2day
3 days
5 days
7 days

Figure 5

Figure 5. Overexpressing CTPS promotes cytoophidium assembly in *H. hispanica*. a, Confocal images of OE-GFP and OE-HhCTPS-GFP in late log phase in AS168 medium. **b**, STED images of OE-GFP and OE-HhCTPS-GFP. **c**, Images of OE-HhCTPS-GFP sampled at different time points. **d**, Growth curve of DF60, OE-GFP and OE-HhCTPS-GFP with a log scale for y axis**.** **e**, **f**, Quantification analysis of images of OE-HhCTPS-GFP for abundance of compartmentalized structure and cell size. Mean ± SD in (**d**), Mean with 95% CI in (**e**). n=1210 for 6 h, 1247 for 1 day. 1378 for 2 days, 1540 for 3 days, 1961 for 5 days, and 1938 for 7 days in (**d**). n= 814 for 6 h, 478 for 1 day. 619 for 2 days, 740 for 3 days, 1230 for 5 days, and 1330 for 7 days in (**e**). Scale bars, 5 μm in (**a**), 2 μm in (**c**).

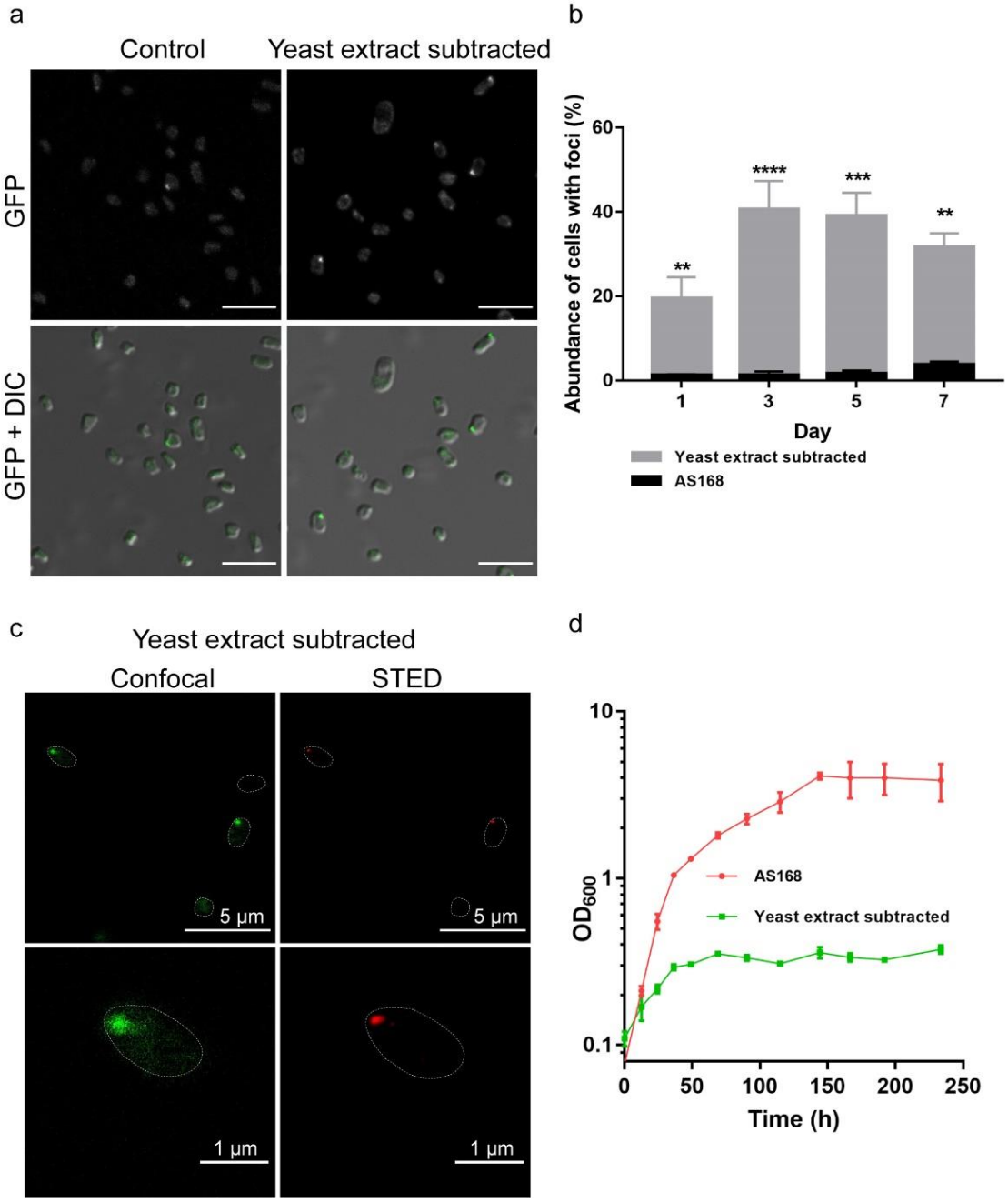
a
Control
Yeast extract subtracted
GFP
GFP + DIC
b
Abundance of cells with foci (%)
60
40
20
0
****
***
**
**
1
3
5
7
Day
Yeast extract subtracted
AS168
c
Yeast extract subtracted
Confocal
STED
5 µm
5 µm
1 µm
1 µm
d
10
1
0.1
OD600
AS168
Yeast extract subtracted
0
50
100
150
200
250
Time (h)

Figure 6

Figure 6. Uracil deprivation affects cytoophidium formation in *H. hispanica.*

a, **c**, Confocal images (**a**) and STED images (**c**) of HhCTPS-GFP in normal and yeast extract subtracted AS-168 on the third day of cultivation. **b**, Quantification of the cells contain compartmentalized structure. N = 985 for 1 day, 1322 for 3 days, 1445 for 5 days, and 1259 for 7 days in AS168. N = 1316 for 1 day, 1436 for 3 days, 1042 for 5 days, and 1172 for 7 days in yeast extract substrate AS168. Mean ± SD. **d**, Growth curve of HhCTPS in normal and yeast extract subtracted AS-168 with a log scale for y axis. Scale bars, 5 μm in (**a**) and upper pane of (**c**). 1 μm in lower pane in (**c**).